Phase transitions and chemical transformations of nitromethane up to 350 °C and 35 GPa

Stéphane Courtecuisse, François Cansell, Denise Fabre, Jean-Pierre Petitet

RESEARCH ARTICLE | JANUARY 08 1995

Phase transitions and chemical transformations of nitromethane up to 350 °C and 35 GPa

Stéphane Courtecuisse; François Cansell; Denise Fabre; Jean-Pierre Petitet

J. Chem. Phys. 102, 968–974 (1995)
https://doi.org/10.1063/1.469165

Phase transitions and chemical transformations of nitromethane up to 350 °C and 35 GPa

Stéphane Courtecuisse
C.E.A. - C.E.V.M., 77181 Courtry Cedex, France

François Cansell, Denise Fabre, and Jean-Pierre Petitet
Laboratoire d'Ingénierie des Matériaux et des Hautes Pressions, C.N.R.S. Institut Galilée, Université Paris-Nord, Avenue Jean-Baptiste Clément, 93430 Villetaneuse, France

(Received 27 July 1994; accepted 26 September 1994)

Nitromethane has been studied as a model of the energetic nitro compounds. The phase diagram has been determined by Raman scattering in the pressure and temperature ranges of 0–35 GPa and 20–350 °C, respectively. Three new solid phases of nitromethane called III, IV, V, and their domain of stability have been located. A first chemical transformation is observed by the disappearance of nitromethane Raman modes and by the irreversible formation of a transparent solid called compound I (CI). A second chemical transformation [compound I–compound II (CII)], at higher temperature than the first one, is observed by the sudden darkening of the sample. © *1995 American Institute of Physics.*

I. INTRODUCTION

Nitromethane is the simplest energetic nitro compound and a usual monopropellant. As such, it has often been chosen as a model for studies of the effect of high pressures and high temperatures on the decomposition reaction. An understanding of the initiation of the deflagration processes could be helped by the knowledge of the microscopic structure, the macroscopic arrangement, and their pressure dependence. That is the reason why a study of the phase diagram appears to be a preliminary stage to deal with a study of the violent decomposition phenomena.

Many studies on the pressure and/or temperature behavior of nitromethane have been undertaken.[1–9] The crystal structure of solid nitromethane has been solved at 4.2 K and atmospheric pressure by Trevino *et al.*[1] from single crystal x-ray diffraction and neutron powder diffraction data. This structure is orthorhombic with four molecules per cell in space group $P2_12_12_1$. The liquid–solid transition has been located at 0.4 GPa and ambient temperature and evidenced up to 160 °C.[2] At room temperature the solid I structure is the same up to 3.5 GPa (Ref. 3) characterized by the free rotation of the methyl group. Between 3.5 and 6 GPa the solid II structure is still the same but the methyl group appears to be fixed and rotated about 45° from its position at the low temperature atmospheric pressure form.

The chemical reaction of nitromethane takes place very slowly at temperature between 100 and 130 °C, and more rapidly at 150 °C for pressures from 2 to 5 GPa.[4] Recently, Agnew *et al.* reported a P-T diagram up to 20 GPa and 280 °C.[5] Their diagram confirmed fast, slow, and no reaction ranges of the nitromethane transformation. In order to fine tune the phase diagram of nitromethane, we report a study performed by Raman spectroscopy up to 35 GPa and 350 °C. From our experimental results three new phase transitions are reported in the P-T diagram. Moreover, two decomposition lines have been determined and two domains of chemical transformed compounds (CI and CII) have been determined. CI is obtained from nitromethane with a low transformation rate (several hours). The second compound (CII) at high temperature is obtained with a higher transformation rate than CI (some minutes).

II. EXPERIMENTAL METHOD

The experiments have been performed in a high pressure membrane type diamond anvil cell[10] made of refractory alloy. The pressure was monitored by a pneumatic ram connected to a pressure generator through a high pressure flexible capillary. The stainless-steel gasket had an aperture of 0.15 mm in diameter and 0.15 mm in depth. This depth was chosen in order to get a sufficient signal.

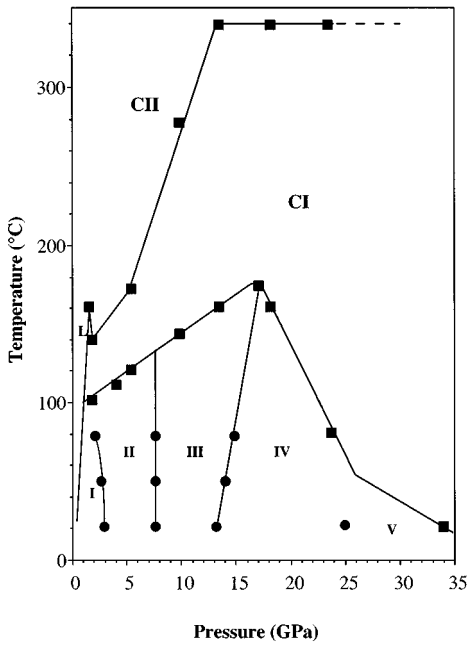

FIG. 1. Phase diagram of nitromethane. The melting curve is from Ref. 2.

 0021-9606/95/102(2)/968/7/$6.00

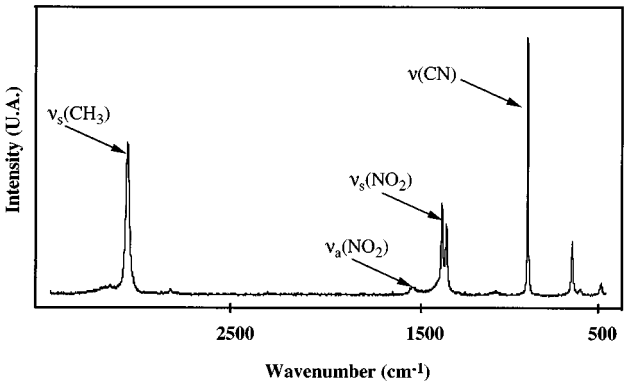

FIG. 2. Raman spectrum of liquid nitromethane at ambient pressure and temperature.

The heater was a coil, which was held up around the cell by a stainless-steel protection jacket. Thanks to the high thermal conductivity of diamond, the temperature homogeneity in the sample may be assumed and a thermocouple measured the temperature on the metallic gasket in contact with the diamond.

The pressure was determined by the pressure shift of the $^5D_0-^7F_0$ singlet (685.4 nm at 0.1 MPa) of $SrB_4O_7:Sm^{2+}$ chips set inside the high pressure chamber.[11] The Sm^{2+} pressure sensor presents the following two advantages in comparison with the ruby: (i) $SrB_4O_7:Sm^{2+}$ has a well-isolated single fluorescence peak, whereas the R_1 line of the ruby belongs to a doublet and the accuracy of the measurement is reduced at high temperature by the broadening and overlap of the two lines of the doublet; (ii) the temperature effects on the position and linewidth of the Sm^{2+} fluorescence peak are small (-0.0001 nm/°C). However, the pressure shift is smaller than that of the ruby ($+0.25$ nm/GPa and $+0.36$ nm/GPa): the accuracy of the pressure measurement is greater with the ruby at ambient temperature. As our experimental method needs a small temperature coefficient, we prefer to use the Sm^{2+} pressure sensor for experiments with temperature.

Raman experiments were carried out in backscattering configuration with an argon ion laser at the 514.5 nm wavelength. The laser power was about 50 mW in order to avoid any thermal or photochemical effect and was focused on the sample with an objective of 15 mm working distance. The frequencies were measured with a multichannel spectrometer DILOR XY. Plasma lines were used for the frequency calibration. According to the observed mode the resolution was from 4 to 10 cm^{-1}. The laser light was vertically polarized and the scattering light was not analyzed.

TABLE I. Studied Raman vibrational modes (cm^{-1}) of nitromethane.

Mode	CH_3NO_2
A_1 $\nu_s(CH_3)$	2955
$\nu_s(NO_2)$	1402
$\nu(CN)$	917
B_1 $\nu_a(NO_2)$	1561

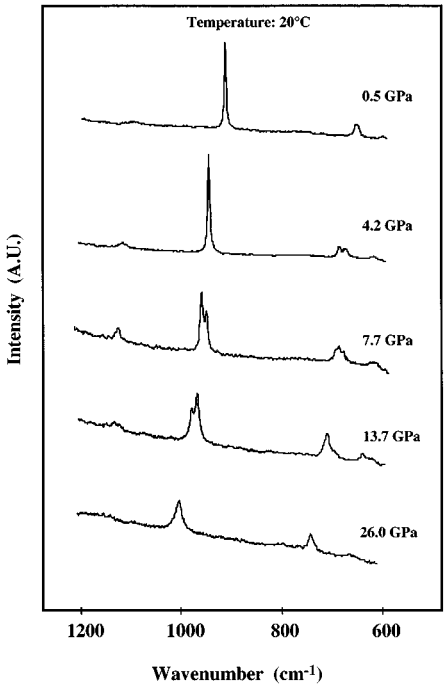

FIG. 3. Raman spectra of the nitromethane A_1 $\nu(CN)$ mode in different phases at ambient temperature.

Measurements have been performed at constant temperature and variable pressure. Since the first chemical transformation rate is low and the solid–solid phase transitions are sluggish, the sample was maintained during several hours for each step of the experimental parameters, before another measurement was made. Nitromethane samples were from

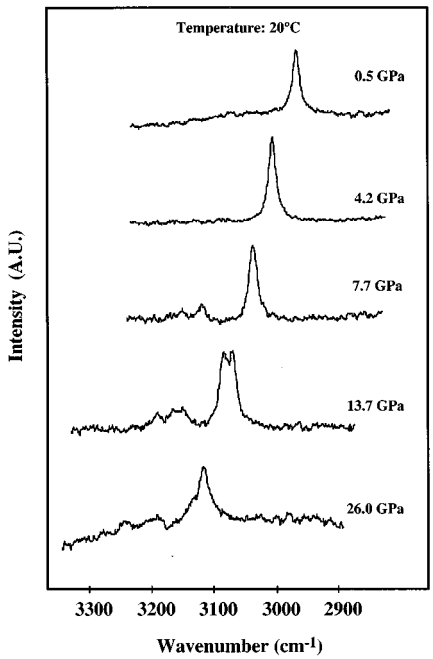

FIG. 4. Raman spectra of the nitromethane A_1 $\nu_s(CH_3)$ mode in different phases at ambient temperature.

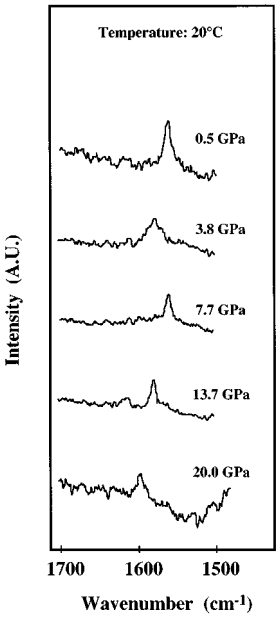

FIG. 5. Raman spectra of the nitromethane B_1 $\nu_a(NO_2)$ mode in different phases at ambient temperature.

commercial purchase (ALDRICH 99+%) and were used without further purification.

III. RESULTS

The P-T diagram of nitromethane has been determined (Fig. 1) by the study of the shift of different Raman modes. The Raman spectrum of liquid nitromethane between 500 and 3500 cm^{-1} is reported in Fig. 2. The assignment of fundamental vibrational bands in the liquid state is given in Table I from Miller *et al.*[12] The Raman spectra of the different phases of nitromethane are reported in Figs. 3, 4, and 5 for the A_1 ν(CN), A_1 $\nu_s(CH_3)$, and B_1 $\nu_a(NO_2)$ modes, respectively.

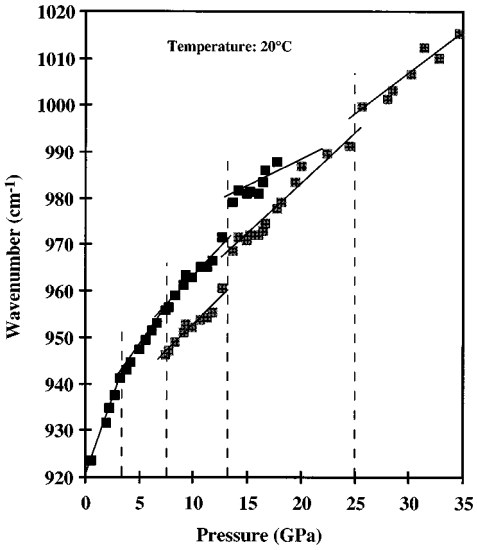

FIG. 6. Effect of pressure on the A_1 ν(CN) mode of nitromethane at ambient temperature.

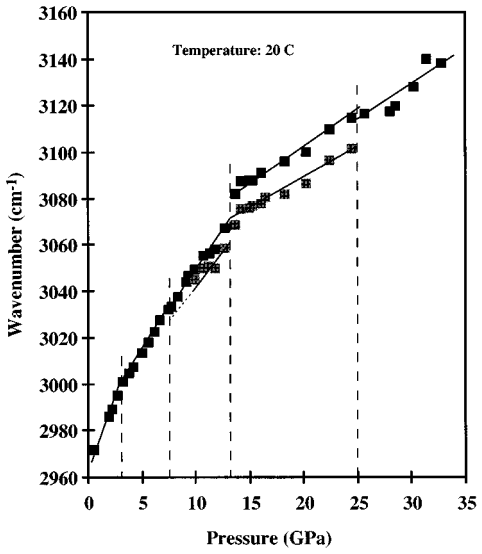

FIG. 7. Effect of pressure on the A_1 $\nu_s(CH_3)$ mode of nitromethane at ambient temperature.

A. Solid transitions of nitromethane

1. Solid I–solid II transition

A transition is located at 3 ± 0.2 GPa at ambient temperature. It is detected by a break in the slope of the pressure dependence of the A_1 ν(CN) (Fig. 6) and A_1 $\nu_s(CH_3)$ (Fig. 7) vibrational frequencies and by a discontinuity in the slope of the B_1 $\nu_a(NO_2)$ mode curve (Fig. 8). The discontinuity of the linewidth (Γ_{NO}) of the B_1 $\nu_a(NO_2)$ mode vs pressure (Fig. 10) confirms unambiguously the transition. The solid I–solid II transition line does not run parallel to the temperature axis (Table II and Fig. 1). At 80°C the transition is located at 2 ± 0.5 GPa.

2. Solid II–solid III transition

The solid II–solid III transition is located at 7.5 ± 0.5 GPa at ambient temperature. It is detected by the appearance of three new bands (Figs. 3, 6, 7, and 9) and by a discontinuity in the B_1 $\nu_a(NO_2)$ mode frequency variations vs pressure (Fig. 8). The discontinuity of Γ_{NO} and the break in the linewidth (Γ_{CH}) of the A_1 $\nu_s(CH_3)$ mode vs pressure

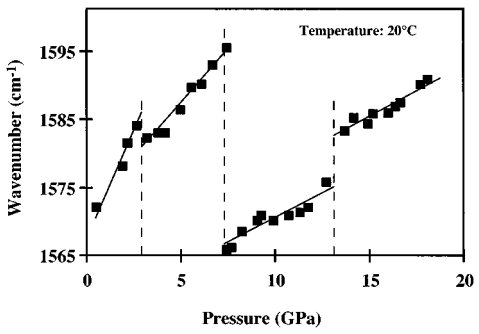

FIG. 8. Effect of pressure on the B_1 $\nu_a(NO_2)$ mode of nitromethane at ambient temperature.

TABLE II. Coordinates of experimental points on the solid I–solid II transition line.

P (GPa)	3	2.8	2
T (°C)	20	50	80

confirm the transition (Figs. 10 and 11). The nitromethane solid II–solid III transition line runs parallel to the temperature axis up to the decomposition line at 130 °C (Table III and Fig. 1).

3. Solid III–solid IV transition

The solid III–solid IV transition is located at 13.2±1 GPa at ambient temperature. The observed discontinuities of the A_1 ν(CN) (Fig. 6), A_1 $\nu_s(CH_3)$ (Fig. 7), B_1 $\nu_a(NO_2)$ (Fig. 8) modes and the break in the slope of the A_1 $\nu_s(NO_2)$ mode shift vs pressure (Fig. 9) confirm the existence of this transition. It is attended with an inversion of the intensity of the A_1 ν(CN) vibrational mode (Fig. 3). The new observed band (Fig. 4) arises only from a different pressure coefficient of the components, which are present since 7.5 GPa but not resolved on account of experimental conditions (see Fig. 7). The break in the behavior of Γ_{NO} (Fig. 10) and the discontinuity in the Γ_{CH} behavior vs pressure (Fig. 11) confirm this transition. The slope of the nitromethane III–IV transition line appears to be positive and reaches the chemical transformation line at 17±1 GPa and 175±10 °C (Table IV and Fig. 1).

4. Solid IV–solid V transition

A transition is detected at 25±1 GPa at ambient temperature by the discontinuities in the evolution of the A_1 ν(CN) (Fig. 6) and the A_1 $\nu_s(NO_2)$ (Fig. 9) modes vs pressure.

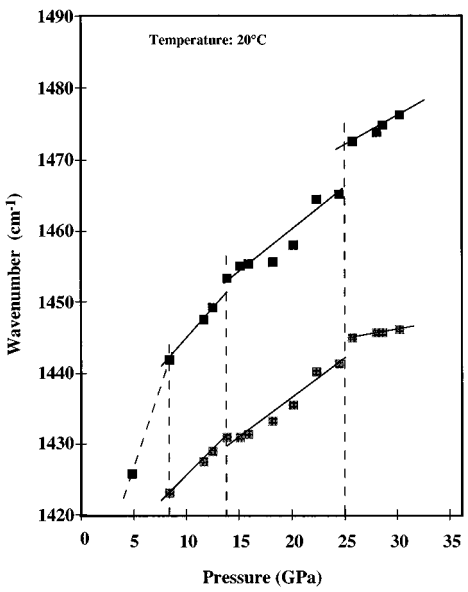

FIG. 9. Effect of pressure on the A_1 $\nu_s(NO_2)$ mode of nitromethane at ambient temperature.

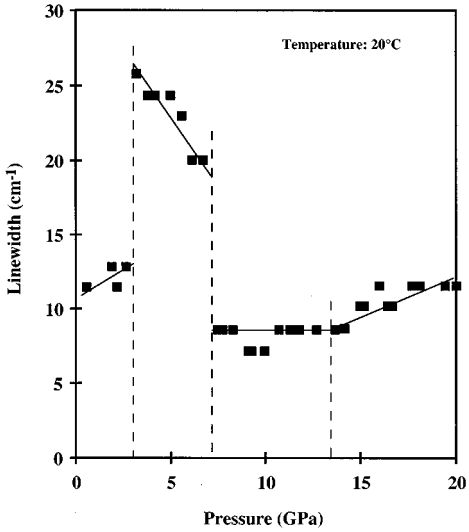

FIG. 10. Evolution of the linewidth (Γ_{NO}) of the nitromethane B_1 $\nu_a(NO_2)$ mode at ambient temperature. The spectral resolution is 7 cm^{-1}.

The nitromethane IV–V transition has not been studied at higher temperature because of the vicinity of the nitromethane transformation at 50 °C for 25 GPa.

B. Chemical transformations of nitromethane

Up to 34 GPa at ambient temperature no decomposition has been observed and the recovered product at ambient pressure shows no modification of the reference spectrum at atmospheric pressure. At 100 °C and 2 GPa nitromethane is transformed after about 10 h. The transformation temperature of nitromethane increases vs pressure up to 175 °C and 17 GPa (Table V and Fig. 1). From solid IV the transformation temperature of nitromethane decreases when pressure increases (Table V and Fig. 1). At room temperature from solid V the chemical transformation occurs at 34 GPa. This transformed product, called CI, is transparent. It does not give any

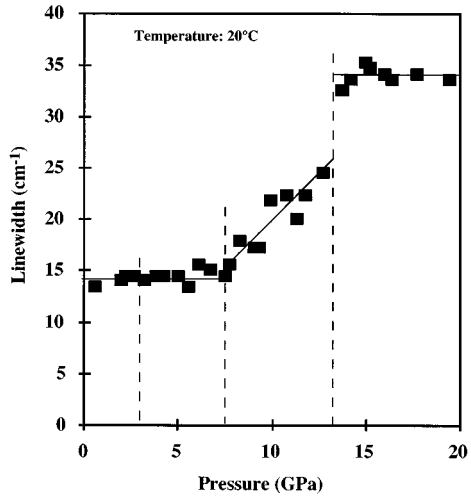

FIG. 11. Evolution of the linewidth (Γ_{CH}) of the nitromethane A_1 $\nu_s(CH_3)$ mode at ambient temperature. The spectral resolution is 10 cm^{-1}.

TABLE III. Coordinates of experimental points on the solid II–solid III transition line.

P (GPa)	7.5	7.5	7.5
T (°C)	20	50	80

TABLE V. Coordinates of experimental points on the solid nitromethane–CI transformation line.

P (GPa)	2	4.2	5.5	10	13.5	17	18.2	23.5	34
T (°C)	100	110	120	145	160	175	160	80	20

Raman signal and the transformation is irreversible. The solid CI compound recovered after releasing the pressure and the temperature persists at ambient conditions.

For a given pressure by temperature raising CI is transformed into a new compound CII (Table VI and Fig. 1). This chemical transformation is characterized by the total absorption of the laser light. The reaction rate is relatively high (only several minutes). The recovered product at ambient pressure does not give any Raman signal. This product shows an orange color by white light transmission and becomes immediately dark when it is lit by the laser beam. The temperature of the CI–CII transformation increases vs pressure up to 340 °C and 13 GPa (Fig. 1). For higher pressures the temperature transformation remains constant at 340 °C.

IV. DISCUSSION

We will discuss successively the solid–solid transitions and the high pressure and high temperature chemical transformations of nitromethane. The solid I–solid II transition located at 3 ± 0.2 GPa at ambient temperature is reported by Cromer *et al.*[2] at 3.5 GPa. The difference in the pressure localization of this transition is due to the fact that Cromer *et al.* worked with too large pressure increments to precisely locate this transition. Indeed they did not make any experiment between 2 and 3.5 GPa. In this work the pressure increments permit to locate with more accuracy the solid I–solid II transition at 3 ± 0.2 GPa. The nitromethane crystal structure between 0.4 and 6 GPa is orthorhombic with four molecules per cell.[1,2] According to Cromer, the transition at 3 GPa corresponds to a blocking of the methyl group rotation.[2] The study of different Raman modes of nitromethane confirmed the fact that the transition solid I–solid II is not strong. Indeed weak changes were observed on the principal vibrational modes (Figs. 6–8). On the other hand, the evolution of Γ_{CH} did not permit to locate this transition. The evolution of Γ_{NO} presents a strong discontinuity (15 cm^{-1}) while Γ_{CH} remains constant (Figs. 10 and 11); this can be interpreted by the fact that the Raman mode (at 1583 cm^{-1} and 20 °C) is the resultant of two components: the first one (1) is the B_1 $\nu_a(NO_2)$ mode and the second one (2) could be a combination band intensified by Fermi resonance with (1) (Fig. 12). The discontinuity in the evolution of the B_1 $\nu_a(NO_2)$ mode vs pressure could be only apparent, in relation to the Fermi resonance (Fig. 12). Indeed the repulsion between the two energy levels in resonance would lead to a lowering of the $\nu_a(NO_2)$ frequency.

At 50 °C and 80 °C the same transition is observed, but it would be located at 2.8 ± 0.2 and 2 ± 0.5 GPa, respectively. This behavior indicates that the transition is activated by an increasing of temperature (Table II).

The solid II–solid III transition is detected by an important modification at 7.5 ± 0.5 GPa in the whole of the studied Raman modes (Figs. 5–11). This transition has not been mentioned by Cromer[2] who worked up to 11.7 GPa. The same explanation as previously given for the solid I–solid II transition can be proposed. Indeed between 8 and 10 GPa no experiment has been performed, but at 10 GPa a splitting of the A_1 ν(CN) mode was observed as in this work. Moreover, we think that the pressure increments must be small (0.5 GPa) and the time-limit between two pressure increments must be higher than 2 h because the solid–solid phase transitions are sluggish.

The splitting of the principal Raman modes [A_1 ν(CN), A_1 $\nu_s(NO_2)$, A_1 $\nu_s(CH_3)$] and the modification of all the Raman modes indicate that the transition is probably a first order structural transition with an increase of the molecules number per cell. Moreover, the high value of the A_1 $\nu_s(NO_2)$ mode splitting (20 cm^{-1}) indicates an important intermolecular coupling in the solid III. As in the case of the transition I–II, the discontinuity in the $\nu_a(NO_2)$ mode pressure evolution would be enhanced by the Fermi resonance between the $\nu_a(NO_2)$ mode and a combination band in phase II. At the end of phase II, where the resonance is stronger, the resulting repulsion between the two vibrational levels leads to a higher frequency than the unperturbed frequency for the $\nu_a(NO_2)$ mode and therefore to an apparent very strong discontinuity. As a matter of fact, even if after a qualitative evaluation of the unperturbed frequency the discontinuity may be reduced from some ten wave numbers, it remains rather strong and indicates a lowering of the energy value of the N–O bond corresponding to a weakening of this bond.

Concerning the linewidth (Γ) behavior of the B_1 $\nu_a(NO_2)$ mode (Fig. 10) vs pressure, the solid II–solid III transition would induce an uncoupling and only the B_1 $\nu_a(NO_2)$ mode would be detected; the other mode would have a weak intensity in agreement with a combination band.

TABLE IV. Coordinates of experimental points on the solid III–solid *IV* transition line.

P (GPa)	13.2	14	15	17
T (°C)	20	50	80	175

TABLE VI. Coordinates of experimental points on the CI–CII transformation line.

P (GPa)	1.6	2	5.5	10	13.5	18.2	23.5
T (°C)	160	140	170	280	340	340	340

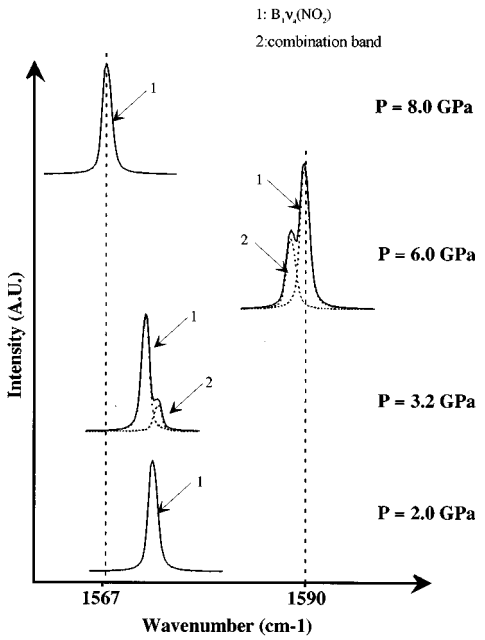

FIG. 12. Schema of the evolution of the nitromethane B_1 $\nu_a(NO_2)$ mode vs pressure at ambient temperature.

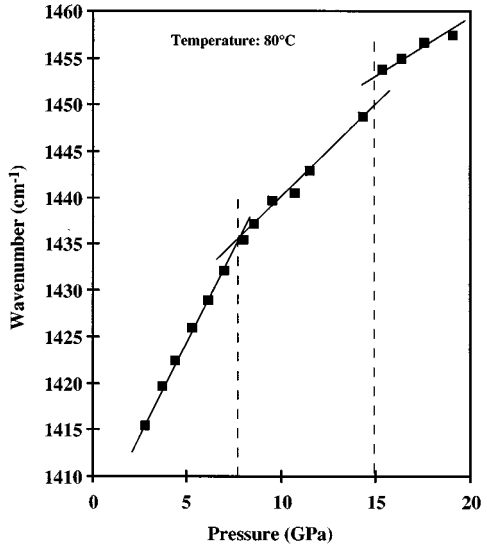

FIG. 14. Effect of pressure on the A_1 $\nu_s(NO_2)$ mode of nitromethane at 80 °C.

Therefore, Γ_{NO} decreases to 15 cm^{-1} at the transition solid II–solid III.

This transition is observed at 50 °C and 80 °C (Figs. 13 and 14) at the same pressure as at ambient temperature, i.e., 7.5±0.5 GPa (Fig. 2). The solid II–solid III line runs parallel to the temperature axis up to the decomposition line (Table III).

The solid III–solid IV transition at 13.2±1 GPa is strongly seen in all the studied vibrational modes vs pressure. This transition is shifted with a temperature change (Table IV). For example, at 80 °C, the solid III–solid IV transition is located at 15±1 GPa.

The solid IV–solid V transition at 25±1 GPa was detected at ambient temperature. The pressure shift of this transition vs temperature has not been studied because nitromethane is transformed as soon as 55 °C are reached. A study at low temperature should be made to determine this transition line evolution.

The nitromethane–CI transformation is an irreversible and slow reaction. Since CI is an amorphous compound its Raman spectrum is not distinguishable from the ground. The chemical transformation curve has to be compared with that of any organic compound, such as benzene.[13] It is important to notice that the slopes of the transformation curve are different (positive and negative respectively) in nitromethane and benzene.

The CI–CII transformation is an irreversible and more rapid reaction than the nitromethane–CI transformation. The reaction is complete when the transformed product is totally dark. The color of CII, observed by optical microscope, was orange by white light transmission. CII did not give any Raman signal and was not analyzed because of the too small recovered quantity.

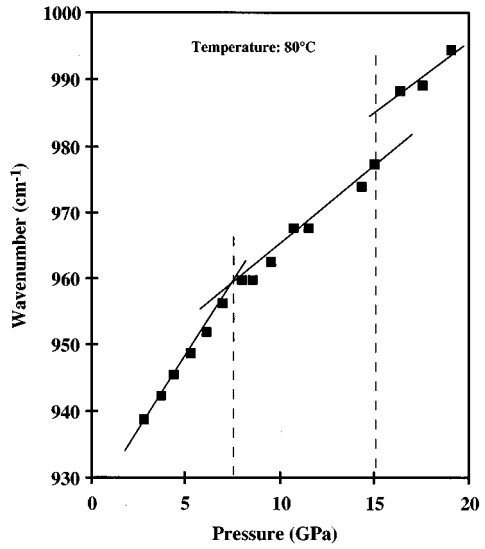

FIG. 13. Effect of pressure on the A_1 ν(CN) mode of nitromethane at 80 °C.

V. CONCLUSION

The pressure and temperature dependence of the more intense vibrational Raman modes of solid nitromethane has been studied for the purpose of establishing its phase diagram. The nitromethane compression up to 35 GPa at ambient temperature allowed us to show up four solid—solid transitions, three of which are new—at 7.5, 13.2, and 25 GPa. The second one (at 7.5 GPa) is probably a first order structural transition with an increase of the molecule number per cell. The solid nitromethane temperature study allowed us to show up two transformation zones—nitromethane/CI and CI/CII—and the different solid phase stability domains.

[1] S. F. Trevino, E. Prince, and C. R. Hubbard, J. Chem. Phys. **73**, 2996 (1980).
[2] G. J. Piermarini, S. Block, and P. J. Miller, J. Phys. Chem. **93**, 457 (1989).
[3] D. T. Cromer, R. R. Ryan, and D. Schiferl, J. Phys. Chem. **89**, 2315 (1985).
[4] J. W. Brasch, J. Phys. Chem. **84**, 2085 (1980).
[5] S. F. Agnew, B. I. Swanson, J. Kenney, and I. Kenney, in *Ninth Symposium (Int.) on Detonation* (Office of Naval Research, Portland, Oregon, 1989), p. 421.
[6] L. J. Hillenbrand, Jr. and M. L. Kilpatrick, J. Chem. Phys. **21**, 525 (1953).
[7] T. L. Cottrell, Graham, and T. J. Reid, Trans. Faraday Soc. **47**, 584 (1951).
[8] S. F. Rice and F. Foltz, Combustion and Flame **87**, 109 (1991).
[9] C. P. Constantinou, T. Mukundan, and M. M. Chaudhri, Philos. Trans. R. Soc. Lond. Ser. A **339**, 403 (1992).
[10] R. Letoullec, J. P. Pinceaux, and P. Loubeyre, High Pressure Res. **1**, 77 (1988).
[11] A. Lacam and C. Chateau, J. Appl. Phys. **66**, 366 (1989).
[12] P. J. Miller, S. Block, and G. J. Piermarini, J. Phys. Chem. **93**, 462 (1989).
[13] F. Cansell, D. Fabre, and J. P. Petitet, J. Chem. Phys. **99**, 7300 (1993).